Available online at www.sciencedirect.com
SCIENCE DIRECT®
Mathematical Biosciences 188 (2004) 47–62
Mathematical Biosciences
www.elsevier.com/locate/mbs

Modeling the long-term control of viremia in HIV-1 infected patients treated with antiretroviral therapy

Michele Di Mascio [a], Ruy M. Ribeiro [a], Martin Markowitz [b], David D. Ho [b], Alan S. Perelson [a,*]

[a] *Theoretical Division, Los Alamos National Laboratory, 1 Los Alamos Lab, Los Alamos, NM 87545-0001, USA*
[b] *Aaron Diamond AIDS Research Center, The Rockefeller University, New York, NY 10016, USA*

Received 17 December 2002; received in revised form 19 August 2003; accepted 21 August 2003

Abstract

Highly active antiretroviral therapy (HAART), administered to a HAART-naïve patient, perturbs the steady state of chronic infection. This perturbation provides an opportunity to investigate the existence and dynamics of different sources of viral production. Models of HIV dynamics can be used to make a comparative analysis of the efficacies of different drug regimens. When HAART is administered for long periods of time, most patients achieve 'undetectable' viral loads (VLs), i.e., below 50 copies/ml. Use of an ultrasensitive VL assay demonstrates that some of these patients obtain a low steady state VL in the range 5–50 copies/ml, while others continue to exhibit VL declines to below 5 copies/ml. Interestingly, when patients exhibit continued declines below 50 copies/ml the virus has a half-life of ~6 months, consistent with some estimates of the rate of latent cell decline. Some patients, despite having sustained undetectable VLs, show periods of transient viremia (blips). We present a statistical characterization of the blips observed in a set of 123 patients, suggesting that patients have different tendencies to show blips during the period of VL suppression, that intermittent episodes of viremia have common amplitude profiles, and that VL decay from the peak of a blip may have two phases.
Published by Elsevier Inc.

Keywords: HIV; Modeling; Viral dynamics; AIDS

* Corresponding author.
E-mail address: asp@lanl.gov (A.S. Perelson).

0025-5564/$ - see front matter Published by Elsevier Inc.
doi:10.1016/j.mbs.2003.08.003

1. Introduction

The quantitative analysis of HIV-1 infection was made possible in 1993 with the development of a quantitative assay for HIV-1 RNA in blood [1,2]. Because each HIV-1 virus particle or virion contains two RNA molecules, this assay allowed the use of HIV-1 RNA as a surrogate for virus particles. The mathematical interpretation of changes in the level of HIV-1 RNA (the viral load) during antiretroviral therapy demonstrated for the first time that despite the fact that HIV-infection generally takes about 10 years to lead to AIDS, rapid dynamics on the time scale of days underlies HIV-1 infection [3,4]. This observation stimulated modeling work, aimed at interpreting experimental data, and led to the development of a new field of study called 'viral dynamics' [5]. Here we review some basic models and provide insights into the events that occur in patients treated for long periods of time with anti-HIV drugs.

Basic models of viral dynamics describe the interaction between cells susceptible to infection (target cells), infected cells and virus. The most common model being

$$\begin{aligned} \frac{\mathrm{d}T}{\mathrm{d}t} &= \lambda - dT - kVT, \\ \frac{\mathrm{d}T^*}{\mathrm{d}t} &= kVT - \delta T^*, \\ \frac{\mathrm{d}V}{\mathrm{d}t} &= pT^* - cV, \end{aligned} \tag{1.1}$$

where T represents target cells, mostly CD4+ T cells, T^* represents infected cells, and V virus. Here it is assumed that target cells are created at rate λ, die at rate d per cell, and are infected with rate constant k. Infected cells, T^*, die at rate δ per cell and produce virus at rate p per cell. Free virus is assumed to be cleared at rate c per virion.

Within a few months of infection, patients typically attain a constant or set-point viral load, which is then roughly maintained for years. If we assume that this is a quasi-steady state characterized by $\mathrm{d}V/\mathrm{d}t = \mathrm{d}T^*/\mathrm{d}t = 0$, then one can show that at this steady state $kT = c\delta/p$. In addition, if we assume that an infected cell produces a total of N virus particles during its lifetime, then the average virion production rate $p = N\delta$, since $1/\delta$ is the average lifespan of a productively infected cell. Thus, the quasi-steady state condition, can also be written as $c = NkT$. This also implies, that if T is changing on a slow time scale, then one or more of the parameters must also be slowly changing. Perelson [6] considered the case in which N increased slowly due to evolution of the virus within infected people, thus leading to a slow decline in T. Other models have invoked a time dependent increase in k due to viral evolution or an increase in the immune response, but in general, what determines the viral set-point and the rate of T cell depletion remains controversial, and is the subject of much modeling [7–9].

When an antiretroviral drug, such as a protease inhibitor, which causes infected cells to produce immature virus particles that are non-infectious, or a reverse transcriptase inhibitor, which effectively blocks the successful infection of a cell, are applied to a patient in steady state the viral load falls. To model this fall, the effectiveness of the drug is introduced into the model. The basic model (1.1), then becomes

$$\begin{aligned}
\frac{dT}{dt} &= \lambda - dT - (1-\varepsilon_{RT})kV_I T,\\
\frac{dT^*}{dt} &= (1-\varepsilon_{RT})kV_I T - \delta T^*,\\
\frac{dV_I}{dt} &= (1-\varepsilon_{PI})pT^* - cV_I,\\
\frac{dV_{NI}}{dt} &= \varepsilon_{PI}pT^* - cV_{NI},
\end{aligned} \tag{1.2}$$

where ε_{RT} and ε_{PI} are the efficacies of the reverse transcriptase inhibitor and protease inhibitor, respectively, and V_I and V_{NI}, denote infectious and non-infectious virions, respectively. Perelson et al. [10] analyzed an experiment in which only a protease inhibitor was given and showed that when $\varepsilon_{PI} = 1$, then the viral load is expected to decay as

$$V(t) = V_0 e^{-ct} + \frac{cV_0}{c-\delta}\left[\frac{c}{c-\delta}\{e^{-\delta t} - e^{-ct}\} - \delta t e^{-ct}\right], \tag{1.3}$$

where V_0 is the initial steady state viral load. Eq. (1.3) was then fit to patient data obtained over the first week of therapy and estimates for c and δ were determined [10].

2. Analysis of viral load data from the start of therapy down to 50 HIV-1 RNA copies/ml

When the steady state is perturbed with more potent therapies, consisting of a combination of protease and reverse transcriptase inhibitors, highly active antiretroviral therapy (HAART) [11], the decay of viral load only follows Eq. (1.3) initially and then a new slower second phase of decay is usually observed (Fig. 1(a)). To explain the observed biphasic decay various generalizations of the basic model (1.1) were made. For example, one could incorporate a second population of infected cells, M^*, that died at a slower rate than T^*, which then provided the source of second phase virus. Alternatively, one can model this source as release of viral particles from follicular dendritic cells in lymph nodes and spleen [12,13], as due to activation of latently infected cells into a productively infected state [11], or a combination of these sources. Data fitting cannot distinguish between these mechanisms [11,12], although due to the small number of latently infected cells [14] they seem an unlikely source. Fitting the observed viral load decay to the long-lived cell model led to the estimates that productively infected cells, T^*, decayed with a half-life ($t_{1/2}$) of about 1 day, and the postulated longer-lived infected population, M^*, decayed with a $t_{1/2} = 1$–4 weeks [11].

If one assumes that these two populations of cells are the only sources of virus, the second phase of decay extrapolates to zero residual infected cells in 2–3 years of completely suppressive antiretroviral therapy [11]. Thus, modeling suggested that even though plasma virus tended to become undetectable after about 3 months of therapy, therapy needs to be maintained for at least 2–3 years. However, the ultimate failure of therapy to eradicate the virus in large cohorts of patients treated for much longer than 3 years suggested that either there exists a third very slowly decaying viral reservoir or HAART does not fully suppress on-going viral replication, or both. With ongoing replication, i.e., with ε_{RT} and/or ε_{PI} not equal to one, it is also possible that the viral load reaches a new steady state that is below the threshold of detection of current assays [15].

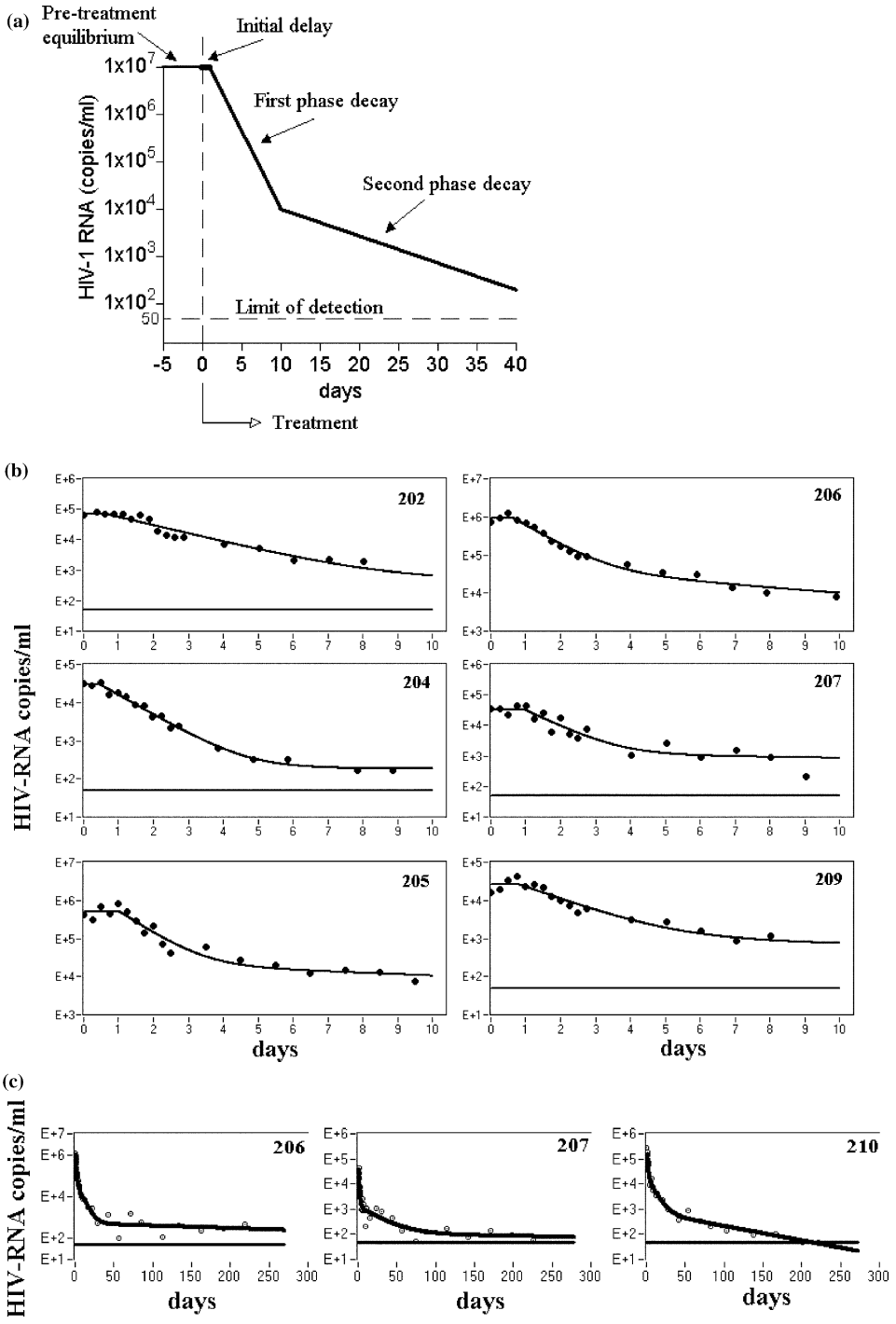

Fig. 1. Plasma HIV-1 RNA decay after initiation of therapy. (a) Typical decay profile. (b,c) Plasma HIV-1 RNA decay in nine HIV-1 infected patients. Theoretical curves (—) were obtained by best-fitting experimental plasma HIV-1 RNA data (○) to Eq. (2.2) using a (b) two or (c) three – compartment model.

Additional slower phases of decay, although postulated, were not observed in these early experiments. However, the existence of an additional reservoir of virus, latently infected cells, has been established [16]. These are cells where the virus has entered, and the viral RNA reverse transcribed into DNA. If this DNA integrates into the cell's chromosome, but is not read out to make new virus particles, the cell is said to be latently infected. Resting CD4+ memory T cells were identified as the latent reservoir [14], and their mean half-life was estimated in different studies as being as short as 6 months [17] or as long as 44 months [18,19]. When latently infected cells are activated they read the viral DNA and may begin viral production, i.e., convert into T^* cells.

A model containing productively infected cells, T^*, long-lived infected cells, M^*, and latently infected cells, L, is given below. The model also incorporates both infectious, V_I, and non-infectious virions, V_{NI} with $V = V_I + V_{NI}$ being the total virus concentration. Delays, τ_{RT} and τ_{PI}, are incorporated to take into account that antiretroviral drugs are not instantly active (pharmacological delay) and that the pharmacological delay for reverse transcriptase inhibitors may be different from that for protease inhibitors.

$$\begin{aligned}
\frac{dT^*}{dt} &= (1-\varepsilon_{RT}h(t-\tau_{RT}))kTV_I + aL - \delta T^*,\\
\frac{dM^*}{dt} &= (1-\varepsilon_{RT}h(t-\tau_{RT}))k_M MV_I - \mu M^*,\\
\frac{dL}{dt} &= (1-\varepsilon_{RT}h(t-\tau_{RT}))fkTV_I - aL - \delta_L L,\\
\frac{dV_I}{dt} &= (1-\varepsilon_{PI}h(t-\tau_{PI}))N\delta T^* + (1-\varepsilon_{PI}h(t-\tau_{PI}))p_M M^* - cV_I,\\
\frac{dV_{NI}}{dt} &= \varepsilon_{PI}h(t-\tau_{RT})N\delta T^* + \varepsilon_{PI}h(t-\tau_{PI})p_M M^* - cV_{NI},
\end{aligned} \tag{2.1}$$

where $h(t-\tau)$ is a Heavyside function, which is 0 for $t < \tau$ and 1 for $t \geqslant \tau$.

In this model we assume for simplicity that the number of uninfected CD4+ T cells (target cells, T) and long-lived cells, M, remain constant during the period of observation. Productively infected cells, T^* and M^*, are generated with rate constants k and k_M, respectively, and produce virus at average rates $N\delta$ and p_M per cell, and are lost with rate constants δ and μ, respectively. Latently infected lymphocytes are generated with rate constant fk, smaller than k by a factor f, are assumed to die with rate constant δ_L and to be activated into productively infected cells with rate constant a, giving a total rate constant of loss $\mu_L = a + \delta_L$. Both infectious and non-infectious virions are cleared with a rate constant c.

Assuming that both reverse transcriptase and protease are completely inhibited by the antiretroviral regimen ($\varepsilon_{RT} = \varepsilon_{PI} = 1$), that $\tau_{RT} = \tau_{PI} = \tau$, and that the system was at steady state before treatment, with baseline viral load V_0, the level of plasma virus after drug therapy is predicted to decay as [11]

$$V(t) = V_0[A\,e^{-\delta(t-\tau)} + B\,e^{-\mu_L(t-\tau)} + C\,e^{-\mu(t-\tau)} + (1-A-B-C)\,e^{-c(t-\tau)}], \tag{2.2}$$

where

$$A = \frac{NkT}{c-\delta}\left(1 - \frac{af}{\delta-\mu_L}\right); \quad B = \frac{af\delta NkT}{\mu_L(\delta-\mu_L)(c-\mu_L)}; \quad C = \frac{c - NkT\left(1+\frac{af}{\mu_L}\right)}{c-\mu}.$$

When $f = 0$, no latently infected T cells are generated and the solution reduces to one for a model with the second phase being generated solely by long-lived cells ($B = 0$).

Eq. (2.2) was used to fit the viral load data obtained in nine chronically HIV-1 infected individuals, treated with a novel potent four-drug combination including both RT and PI drugs (Quad regimen). The value of c was fixed at 23 d^{-1}, a value previously estimated from an experiment not involving drug therapy [20], and the remaining parameters were estimated. Six out of nine patients showed viral load over the threshold of 50 copies/ml for a period of less than three months from the start of therapy (Fig. 1(b)), whereas the remaining three patients showed viral load over the threshold for a period of more than 7 months from the start of therapy (Fig. 1(c)). For these latter three patients the viral load data demonstrates a third phase of decay and Eq. (2.2) was used to fit the experimental data with $f \neq 0$, whereas for the former six patients the model with $f = 0$ was used.

We estimated that the mean death rate of productively infected cells, δ, was 1.0 ± 0.3 d^{-1} and the mean death rate of long-lived cells, μ, was 0.04 ± 0.03 d^{-1} [21]. Comparing these estimates with previous estimates obtained in a group of 8 HIV-1 infected patients treated with a less potent regimen of antiretroviral drugs [11], we observe no difference in the estimate of μ, but a statistically significant difference in δ ($\delta = 1.0 \pm 0.3$ d^{-1} in the Quad regimen, versus $\delta = 0.7 \pm 0.2$ d^{-1} in a three drug regimen [11], Mann–Whitney test, $P = 0.012$).

From the biology of the system, the death rate of productively infected cells is not expected to depend on the drug regimen. The solution (2.2) was obtained with the simplifying assumption $\varepsilon_{RT} = \varepsilon_{PI} = 1$, i.e., 100% effectiveness of the drugs. If we remove this assumption, we can show that the slope of the first phase of plasma HIV-1 decay is approximately given by $\varepsilon'\delta$, the product of the death rate of productively infected CD4+ T cells and the total drug efficacy, where $(1 - \varepsilon') = (1 - \varepsilon_{RT})(1 - \varepsilon_{PI})$ [22]. By assuming $\delta = 1.0$ d^{-1}, the value obtained in the Quad regimen group, as the more reliable estimate of the death rate of productively infected cells, since the assumption of optimal therapy is more closely satisfied, we can then compute the efficacies of other less complex drug regimens relative to the Quad regimen [23].

3. Analysis of viral load data below 50 HIV-RNA copies/ml in HAART treated patients

Almost all recent experimental data on viral load (VL) decay has been obtained with assays that have a lower limit of detection of 50 copies/ml. Recently, new super-sensitive reverse transcriptase–polymerase chain reaction assays that can quantitate viral load in the plasma to 5 copies/ml were developed and used in a research setting to quantitate plasma virus levels [24]. Moreover, this new assay can also detect if at least one amplifiable viral genome is present in the sample.

In collaboration with R. Pomerantz, Thomas Jefferson University Medical Center, Philadelphia, PA, data from five HIV-1-infected men were analyzed with the super-sensitive assay [25]. These patients were a special subset of a larger group of HAART treated patients, who not only had plasma viral RNA levels < 50 copies/ml but were also known to be adherent to their HAART therapy and who had no intercurrent illnesses. We felt that this subset of patients best represented patients with little or no viral replication for whom we might be able to discern continuing plasma virus decay.

Viral load data were fit using a maximum likelihood procedure that allowed for 'censored data' [26], i.e., that took into account that some plasma VL values were below the quantitative threshold of 5 copies/ml or the qualitative threshold of 1 copy/ml. In some samples no viral transcripts could be detected, and were treated as < 1 copy/ml. In all five patients we observed a decay of VL over time, and in three patients the decay slope, m, was significantly different from 0. In Fig. 2 the data and the regression lines, when significant, are shown for each of these patients. The corresponding half-lives ($t_{1/2}$) were computed from the estimate of m, $t_{1/2} = \ln 2/m$. The decay slope was statistically different from zero only for patients 1, 2 and 5 ($P < 2.6 \times 10^{-3}$). For these patients the plasma viral load decay yielded half-lives of 256, 149 and 138 days, respectively, with a mean of approximately 6 months [25].

Although the study involved only five patients, it seems relevant that the estimated mean half-life of 6 months is the same as the estimated half-life of latently infected cells in individuals consistently maintaining plasma HIV-1 RNA levels of fewer than 50 copies/ml [17,18]. Patients 3 and 4 did not show significant plasma viral load decays. Thus, in these two patients the plasma VL may have reached a new quasi-steady state in which low level viral replication was balanced by

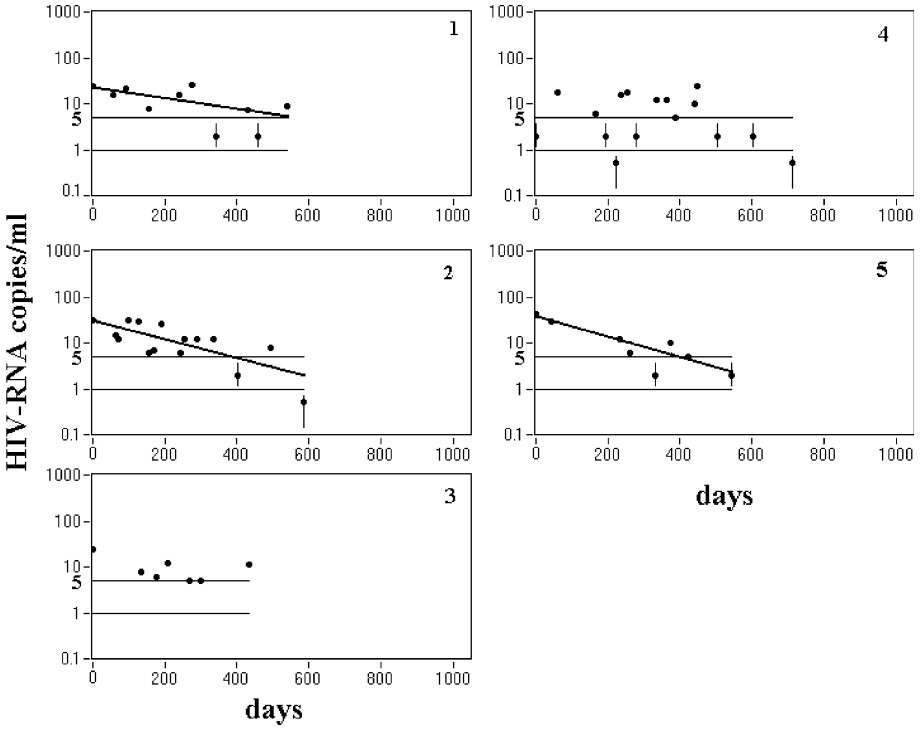

Fig. 2. Plasma HIV-1 RNA viral loads (○) for five HAART treated patients and best- fit linear regression lines. For patients 3 and 4 the slope of the regression line was not statistically different from zero and is not shown. Viral load data were fit using a maximum likelihood procedure that allows for 'censored data', i.e., data given in the form of <5 copies/ml or <1 copy/ml. We assume values reported as <5 copies/ml are between 1 and 5 copies/ml, thus the data points have associated vertical bars. Similarly, a measurement of 0 is here reported as anything below 1 copy/ml and a vertical bar indicates this uncertainty.

viral clearance or be so close to steady state that the rate of viral decay could not be reliably established. The existence of such low viral steady states was suggested by the work of Furtado et al. [27], in which constant low levels of *tat*, *rev* and *gag* messenger RNA were detected in HAART treated patients with plasma viral loads below 50 copies/ml, and are predicted by dynamic models of HIV-1-infection and treatment in which drug sanctuaries exist [15].

4. Analysis of the occurrence of viral blips in HAART treated patients during the period of viral load suppression

In patients treated with potent antiretroviral therapies, viral loads are frequently driven below the usual assay limit of 50 copies/ml. When such patients are repeatedly tested, VLs tend to stay below 50 copies/ml but on occasion a value above threshold is obtained. These occasional measurements above 50 copies/ml are commonly called 'blips'. At first, blips were thought to represent assay errors. However, as we show below, in most patients analysis of blip time series indicates that this is not the case, and that blips represent a transient episode of elevated viremia. Thus, viral blips are indicative of increased viral replication and the underlying causes need to be elucidated.

We studied the dynamics of viral blips by analyzing VL data from patients in eight different clinical studies, differing in the combination of drugs used for therapy, with each combination containing both reverse transcriptase and protease inhibitors. Patients started therapy at different times, were tested a different number of times and observed for different lengths of time. The general pattern of VL decay consisted of a fast first phase followed by a slower second phase, after which patients usually had VLs of <50 copies/ml with occasional blips.

We define the period of sustained viral load suppression as starting when two consecutive VL measurements below 50 copies/ml occur and ending at the last VL measurement below threshold. The eight studies involved 175 patients but only 123 patients showed a long enough period of sustained viral load suppression for viral blip analysis. Overall, the 123 selected periods of VL suppression consisted, on average ($\pm$ s.d.), of 26 ± 15 VL measurements taken over a period of 810 ± 468 days. Some of the analyses described below were repeated in a 'homogeneous subgroup' of 33 patients with a similar number of VL tests and times of observation (within 25% of the group's mean), in order to reject spurious results that might arise from non-homogeneity of sampling or amount of data.

The mean and median frequencies of viral blips in the 123 patients were 0.09 and 0.06/sample, respectively. The blip frequency distribution among the 123 patients, plotted in Fig. 3(a), indicates that the majority of patients show low values of blip frequency. The distribution of frequencies observed in the homogeneous subgroup is shown in Fig. 3(b) and resembles well the one for the total population of patients. In the homogeneous subgroup the mean and median frequencies of viral blips were 0.08 ± 0.10 and 0.05/sample, respectively, and the mean number of VL measurements per patient was 31 ± 4.

We now ask if this frequency distribution can be obtained by assuming that viral blips are independent events, both among patients and for a given patient, and follow a common time-invariant probability distribution. Under these assumptions there will be a theoretical probability, p_s, for a given patient to show s blips. If patients were tested the same number of times, $\bar{n}$, we can

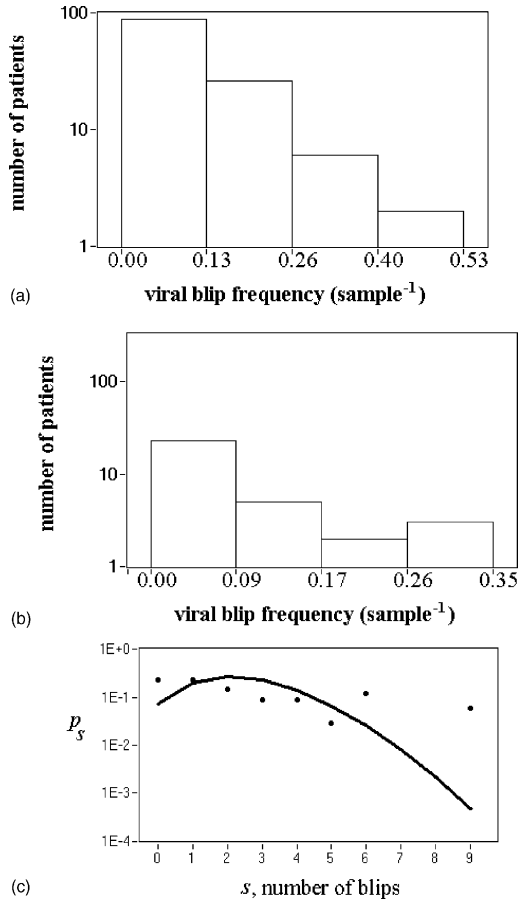

Fig. 3. Viral blip frequency. (a) Distribution of viral blip frequencies in the total patient population. The histogram was obtained by subdividing the range of observed blip frequencies per patient into four subintervals and counting the number of patients having a blip frequency within each subinterval (the extremes of each subinterval are shown on the x-axis). (b) Distribution of viral blip frequencies in the *homogeneous subgroup*. (c) Theoretical probability (—), p_s, of a patient showing s blips, under the assumption that patients have a common probability for exhibiting blips, compared with the observed frequency of patients showing s blips (●).

reject the null hypothesis that patients have the same blip frequency distribution, by comparing the observed fraction of patients showing s blips, f_s, in $\bar{n}$ measurements with the binomial distribution

$$p_s = \binom{\bar{n}}{s} p^s (1-p)^{\bar{n}-s}. \tag{4.1}$$

In the homogeneous-subgroup patients were tested a similar but not necessarily identical number of times. We define ω_n as the fraction of patients tested n times. The distribution of ω_n is unimodal. For simplicity, if we assume that ω_n is binomially distributed with mean $\bar{n}$ and variance σ^2, then the density of ω_n is given by

$$P(\omega_n = \tilde{\omega}_n) = \binom{k}{n} r^n (1-r)^{k-n}, \tag{4.2}$$

where $r = 1 - \frac{\sigma^2}{\bar{n}}$, $k = \frac{\bar{n}}{r}$.

If ω_n is binomially distributed, the following expression for p_s can be derived [28]:

$$p_s(G) = \binom{k}{s} (rG)^s (1-rG)^{k-s}, \tag{4.3}$$

where $G = \frac{1}{n}\sum_{t=1}^{\infty} t f_t$ is the expected value of the fraction of VL measurements that are blips.

In Fig. 3(c) we compare f_s, the fraction of patients showing s blips computed for the homogeneous subgroup, with the theoretical probabilities p_s, computed from (4.3) with $\bar{n} = 31$. We find that some patients have fewer blips and some have more blips than expected. Using a chi-square test, we reject the null hypothesis that patients have a common probability, p, for exhibiting viral blips ($P < 0.05$). Thus, our analysis argues against random events with a fixed probability of occurrence, such as assay variation, being the major cause of blips. Further generalization of Eq. (4.1) where the constraint for ω_n being binomially distributed is removed also leads to the same conclusion [28].

Using a bootstrapping procedure to examine the effects of randomizing the VL time series for each patient, we deduced that blips within one patient obtained by sampling VLs more than 22 days apart appear to be independent events [29], whereas blips less than 22 days apart appear to be part of the same episode of elevated viremia. Thus, when blips are more than 22 days apart they appear to occur independently within patients, but with different frequencies among patients.

The mean and median amplitude of a viral blip in the full dataset were 158 ± 132 and 104 HIV-1 RNA copies/ml, respectively. The distribution of viral blip amplitudes, shown in Fig. 4 for the total group of 123 patients and for the homogeneous subgroup, has an interesting pattern, with most blips having low amplitude and a few blips having large amplitude. The distribution appears to be exponential at low amplitudes but decreases slower than exponentially at high amplitudes.

It is of interest to determine the VL amplitude profile of one of these episodes of elevated viremia. If we assume that intermittent episodes of viremia have a common amplitude profile, then the observed VL amplitude distribution should be generated by randomly sampling the profile characteristic of an episode of elevated viremia (Fig. 6(a)). The existence of a common profile for the viral blips implies that we should observe higher maximum blip amplitudes in patients showing higher numbers of blips, since with greater sampling it is more likely that we observe the maximum of the common profile.

Let A, a continuous random variable, be the amplitude of a viral blip, with probability density function, $\phi(A)$. Let $(x_1, x_2, \ldots, x_n)$ be the n-tuple of blip amplitudes observed for a given patient. Reorder the n-tuple so that $x_{(1)} \leqslant x_{(2)} \cdots \leqslant x_{(n)}$, with $x_{(n)}$ the maximum among the n observed amplitudes. The probability that the maximum among the n observed values is $\leqslant \tilde{A}$, is given by the probability that each amplitude is $\leqslant \tilde{A}$. If we assume that blips are independent events this probability is given by

$$P(x_{(n)} \leqslant \tilde{A}) = \left[\int_0^{\tilde{A}} \phi(A)\, \mathrm{d}A \right]^n. \tag{4.4}$$

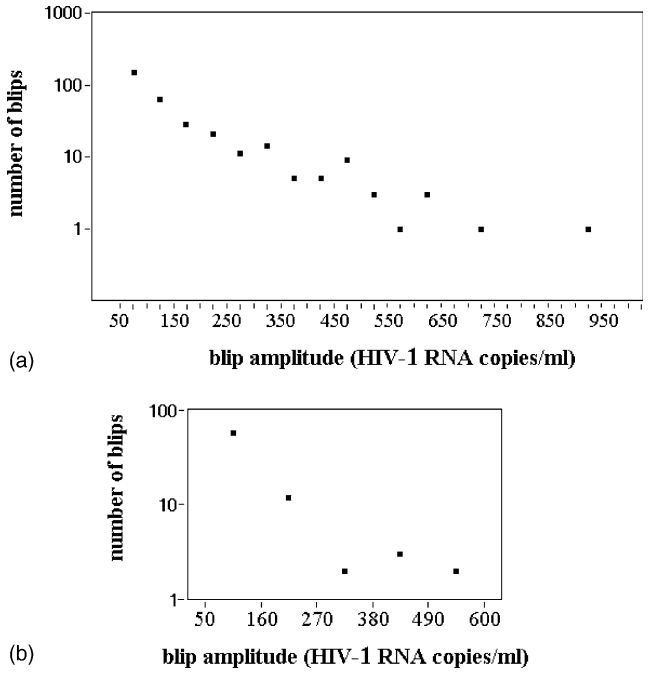

Fig. 4. Viral blip amplitudes. (a) Distribution of the number of blips versus viral blip amplitude in the total population of patients. The histogram was obtained by counting the number of blips (y-axis) with amplitude in each subinterval of 50 HIV-1 RNA copies/ml (the extremes of each subinterval are shown on the x-axis). (b) The same distribution for the homogeneous *subgroup* was built with subintervals of 110 HIV-1 RNA copies/ml.

Differentiating the cumulative distribution, the probability density is given by

$$P(\tilde{A} \leqslant x_{(n)} < \tilde{A} + \mathrm{d}\tilde{A}) = n\left[\int_0^{\tilde{A}} \phi(A)\,\mathrm{d}A\right]^{n-1} \phi(\tilde{A})\,\mathrm{d}\tilde{A}. \tag{4.5}$$

Thus, the expected value of the maximum amplitude among n blips observed in a given patient is

$$E[x_{(n)}] = n\int_0^{\infty} \tilde{A}\left[\int_0^{\tilde{A}} \phi(A)\,\mathrm{d}A\right]^{n-1} \phi(\tilde{A})\,\mathrm{d}\tilde{A}. \tag{4.6}$$

Fig. 5 shows that the observed maximum blip amplitude for patients showing n blips overlap with the theoretical maximum amplitude obtained from (4.6), where the cumulative and density distributions for the random variable A were numerically obtained from the distribution of blip amplitudes. Thus, the null hypothesis that intermittent episodes of viremia have common profiles cannot be rejected based on this observation ($P > 0.05$).

Now, if we assume that the time a VL is measured is random with respect to the VL changes occurring during a blip and that intermittent episodes of viremia have a common profile, then one should be able to generate the observed distribution of viral blip amplitudes by randomly sampling one hypothetical transient episode of viremia. Thus, we investigated different shapes or set of

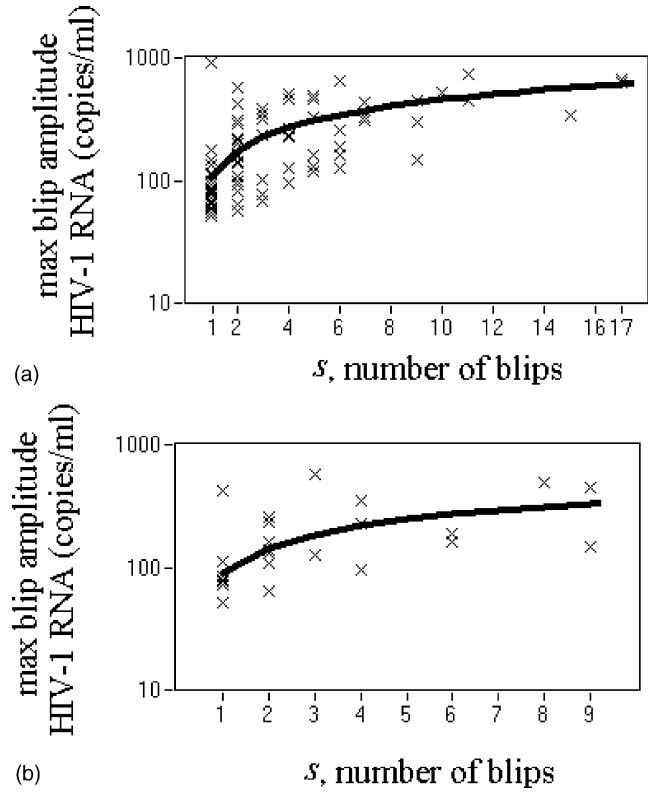

Fig. 5. Maximum viral blip amplitude (×) versus number of blips, s, per patient. The solid line indicates the expected value of the maximum viral blip amplitude for a patient showing s blips under the assumption that intermittent episodes of viremia have a common amplitude profile. (a) The total population of patients. (b) The *homogeneous subgroup*.

shapes for an intermittent episode of viremia that are compatible with the measured amplitude distribution. Although, to our knowledge, no one has ever sampled a patient frequently enough during a blip to know how the viral load changes during a blip, when a patient is put on HAART the viral load decays exponentially in a rapid first phase, followed by a slower second exponential decay. Also, after a therapy interruption, viral loads tend to rise rapidly [30,31]. So we asked what type of amplitude distribution would we obtain if we sampled a blip with decaying exponential viral load.

Fig. 6(b) illustrates a hypothetical blip that has a rapidly rising and then decaying exponential part. To obtain a high VL, say between 400 and 540 copies/ml, the blip would need to be sampled during a $0.3 + 3.1 = 3.4$ day interval, where the two numbers represent the time spent in the rising and falling parts, respectively. However, since the blip profile has a longer flat part, to obtain a low VL measurement, say between 60 and 200 copies/ml, the blip could be sampled during a $1.1 + 11.5 = 12.6$ day interval (Fig. 6(b)). The net result is that, in this example, it would be about 4-fold more likely to observe a low amplitude blip than a high amplitude one. Examining Fig. 4(a), one notices that it is about 10-fold more likely to observe a blip between 60 and 200 copies/ml than one of 400–560 copies/ml. From a preliminary study of examples of this sort, we believe it

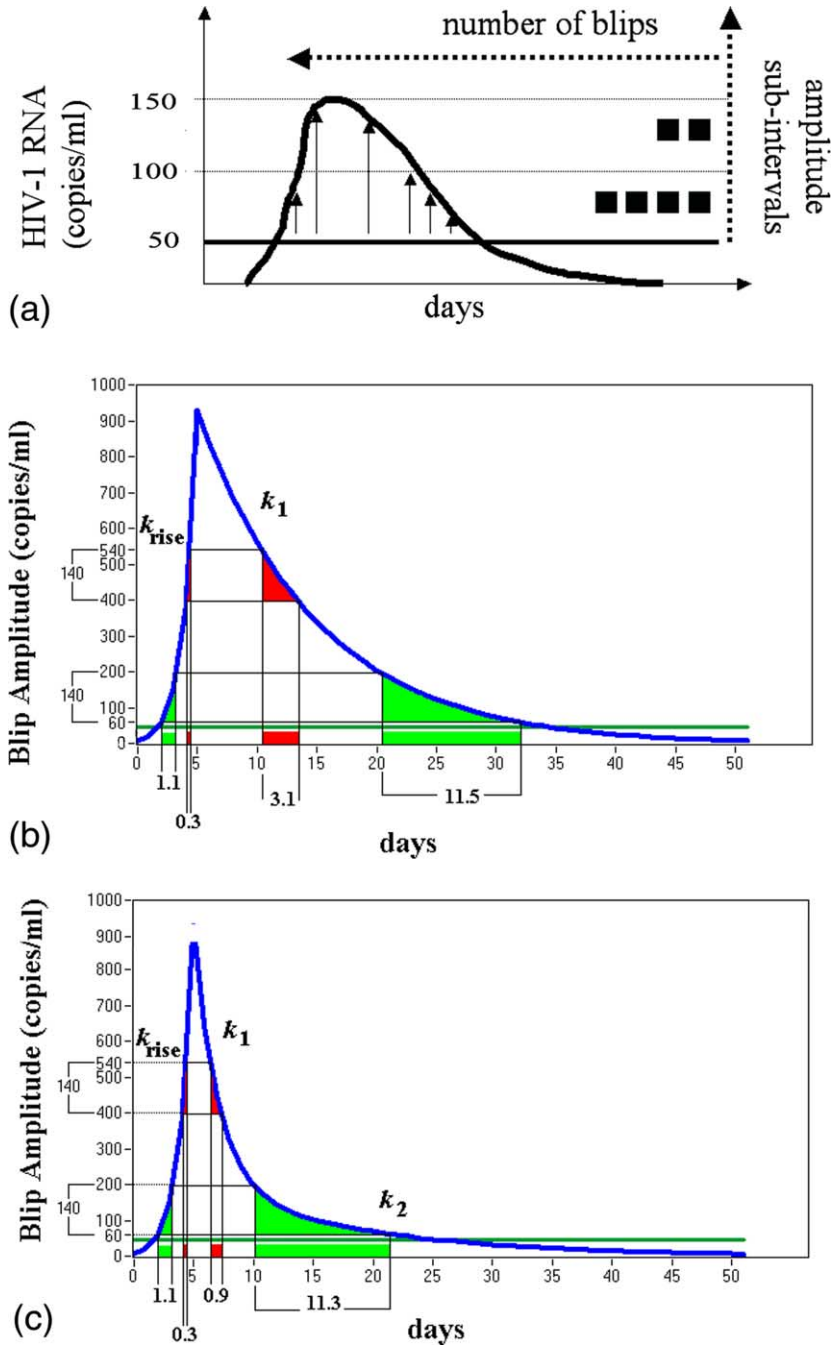

Fig. 6. Hypothetical VL profile for a blip. (a) The distribution of viral blip amplitudes can be theoretically generated by randomly sampling a hypothetical intermittent episode of viremia. (b) A hypothetical profile with an exponentially rising part and a decaying exponential part. (c) A hypothetical profile with a two-phase decay. Notice that if the blip in (b) were sampled randomly it would be about 4-fold more likely to obtain an amplitude between 60 and 200 copies/ml than an amplitude between 400 and 540 copies/ml; for the blip in (c) it would be 10-fold more likely.

unlikely that a blip with a single exponential fall (Fig. 6(b)) can explain the amplitude data in Fig. 4. However, since two phases VL decays are observed after therapy initiation, the blip profile is also likely to have a double exponential decay as shown in Fig. 6(c). Now, with a slow second phase, low amplitude blips are favored, getting closer to the observed amplitude distribution. In fact, for the profile in Fig. 6(c) the ratio between the time spent at low and high amplitudes is about the desired 10:1. Finally, by a non-linear best-fit procedure we estimated the ratio between the decay slopes of the two phases of the hypothetical profile shown in Fig. 6(c) (where we have neglected the contribution of the raising part). We found that the ratio is 9.46 (95% conf. interval: 9.13–9.86). Note that a one order of magnitude difference was also found between the first and second phases of VL decay observed in patients treated with HAART ($\bar{\delta} = 0.70\ d^{-1}$; $\bar{\mu} = 0.07\ d^{-1}$) [11]. If we use the additional information of a mean duration of a transient episode of viremia of about 20–30 days [29], then the two decays constants approach the values of 0.6 and 0.06 d^{-1}, which are similar to the decay constants estimated in previous studies and may reflect the death rates of short and long-lived subpopulations of infected cells [11].

The above results represent a preliminary analysis. However, this kind of analysis should allow us to more accurately deduce a shape, or set of shapes, for a blip that are compatible with the measured amplitude distribution. In mathematical terms we need to solve an 'inverse problem', i.e., deduce from the amplitude distribution the underlying set of blip shapes that generated the given distribution. In general, one cannot find a unique solution to an inverse problem unless additional information is used. Here, the assumption that the decay should be exponential or a sum of exponentials may provide the required additional information.

5. Conclusions

We have previously shown that, in patients under suppressive therapy, the decay of the latent reservoir is inversely correlated with the frequency of viral blips [18]. Here we have provided evidence that in a select set of patients showing no blips it is possible to observe VL decay below 50 copies/ml with a half-life of 6 months, which corresponds to the shortest mean estimated half-life of the latent reservoir [17,19]. We have also shown that blips do not simply represent measurement errors but might arise from similar, transient perturbations of VLs during prolonged treatment, and thus probably occur with common etiology that remains to be determined. However, the fact that blips are observed clearly indicates that virus is persisting despite potent therapy. Uncovering the mechanism of blip generation may provide insights in the requirements for eliminating viral persistence.

Acknowledgements

Portions of this work were performed under the auspices of the US Department of Energy. This work was supported by NIH grants RR06555, AI28433, AI41387, AI41534, the General Clinical Research Center of the Rockefeller University (MO1-RR00102), and the Columbia-Rockefeller Center for AIDS Research (AI42848). We also acknowledge the support of Roche Diagnostics in providing HIV-1 testing materials.

References

[1] M. Piatak Jr., M.S. Saag, L.C. Yang, S.J. Clark, J.C. Kappes, K.C. Luk, B.H. Hahn, G.M. Shaw, J.D. Lifson, Determination of plasma viral load in HIV-1 infection by quantitative competitive polymerase chain reaction, AIDS 7 (Suppl. 2) (1993) S65.

[2] M. Piatak Jr., M.S. Saag, L.C. Yang, S.J. Clark, J.C. Kappes, K.C. Luk, B.H. Hahn, G.M. Shaw, J.D. Lifson, High levels of HIV-1 in plasma during all stages of infection determined by competitive PCR, Science 259 (1749) 1749.

[3] D.D. Ho, A.U. Neumann, A.S. Perelson, W. Chen, J.M. Leonard, M. Markowitz, Rapid turnover of plasma virions and CD4 lymphocytes in HIV-1 infection, Nature 373 (1995) 123.

[4] X. Wei, S.K. Ghosh, M.E. Taylor, V.A. Johnson, E.A. Emini, P. Deutsch, J.D. Lifson, S. Bonhoeffer, M.A. Nowak, B.H. Hahn et al., Viral dynamics in human immunodeficiency virus type 1 infection, Nature 373 (1995) 117.

[5] M.A. Nowak, R.M. May, Virus Dynamics: Mathematical Principles of Immunology and Virology, Oxford University, Oxford, 2000.

[6] A.S. Perelson, in: D. Metlzer (Ed.), Complexity: Metaphors, Models, and Reality, Addison-Wesley, Reading, MA, 1994, p. 185.

[7] V. Muller, A.F.M. Maree, R.J. De Boer, Small variations in multiple parameters account for wide variations in HIV-1 set points: a novel modelling approach, Proc. R. Soc. London B Biol. Sci. 268 (2001) 235.

[8] A.N. Phillips, A. McLean, M.A. Johnson, M. Tyrer, V. Emery, P. Griffiths, M. Bofill, G. Janossy, C. Loveday, HIV-1 dynamics after transient antiretroviral therapy: implications for pathogenesis and clinical management, J. Med. Virol. 53 (1997) 261.

[9] N.I. Stilianakis, K. Dietz, D. Schenzle, Analysis of a model for the pathogenesis of AIDS, Math. Biosci. 145 (1997) 27.

[10] A.S. Perelson, A.U. Neumann, M. Markowitz, J.M. Leonard, D.D. Ho, HIV-1 dynamics in vivo: virion clearance rate, infected cell life-span, and viral generation time, Science 271 (1996) 1582.

[11] A.S. Perelson, P. Essunger, Y. Cao, M. Vesanen, A. Hurley, K. Saksela, M. Markowitz, D.D. Ho, Decay characteristics of HIV-1-infected compartments during combination therapy, Nature 387 (1997) 188.

[12] W.S. Hlavacek, N.I. Stilianakis, D.W. Notermans, S.A. Danner, A.S. Perelson, Influence of follicular dendritic cells on decay of HIV during antiretroviral therapy, Proc. Nat. Acad. Sci. USA 97 (2000) 10966.

[13] W.S. Hlavacek, N.I. Stilianakis, A.S. Perelson, Influence of follicular dendritic cells on HIV dynamics, Philos. Trans., R. Soc. London B 355 (2000) 1051.

[14] T.W. Chun, L. Carruth, D. Finzi, X. Shen, J.A. DiGiuseppe, H. Taylor, M. Hermankova, K. Chadwick, J. Margolick, T.C. Quinn, Y.H. Kuo, R. Brookmeyer, M.A. Zeiger, P. Barditch-Crovo, R.F. Siliciano, Quantification of latent tissue reservoirs and total body viral load in HIV-1 infection, Nature 387 (1997) 183.

[15] D.S. Callaway, A.S. Perelson, HIV-1 infection and low steady state viral loads, Bull. Math. Biol. 64 (2002) 29.

[16] D. Finzi, M. Hermankova, T. Pierson, L.M. Carruth, C. Buck, R.E. Chaisson, T.C. Quinn, K. Chadwick, J. Margolick, R. Brookmeyer, J. Gallant, M. Markowitz, D.D. Ho, D.D. Richman, R.F. Siliciano, Identification of a reservoir for HIV-1 in patients on highly active antiretroviral therapy, Science 278 (1997) 1295.

[17] L. Zhang, B. Ramratnam, K. Tenner-Racz, Y. He, M. Vesanen, S. Lewin, A. Talal, P. Racz, A.S. Perelson, B.T. Korber, M. Markowitz, D.D. Ho, Quantifying residual HIV-1 replication in patients receiving combination antiretroviral therapy, New England J. Med. 340 (1999) 1605.

[18] B. Ramratnam, J.E. Mittler, L. Zhang, D. Boden, A. Hurley, F. Fang, C.A. Macken, A.S. Perelson, M. Markowitz, D.D. Ho, The decay of the latent reservoir of replication-competent HIV-1 is inversely correlated with the extent of residual viral replication during prolonged anti-retroviral therapy, Nat. Med. 6 (2000) 82.

[19] D. Finzi, J. Blankson, J.D. Siliciano, J.B. Margolick, K. Chadwick, T. Pierson, K. Smith, J. Lisziewicz, F. Lori, C. Flexner, T.C. Quinn, R.E. Chaisson, E. Rosenberg, B. Walker, S. Gange, J. Gallant, R.F. Siliciano, Latent infection of CD4+ *T* cells provides a mechanism for lifelong persistence of HIV-1, even in patients on effective combination therapy, Nat. Med. 5 (1999) 512.

[20] B. Ramratnam, S. Bonhoeffer, J. Binley, A. Hurley, L. Zhang, J.E. Mittler, M. Markowitz, J.P. Moore, A.S. Perelson, D.D. Ho, Rapid production and clearance of HIV-1 and hepatitis C virus assessed by large volume plasma apheresis, Lancet 354 (1999) 1782.

[21] M. Markowitz, M. Louie, A. Hurley, E. Sun, M. Di Mascio, A.S. Perelson, D.D. Ho, A novel antiviral intervention results in more accurate assessment of human immunodeficiency virus type 1 replication dynamics and *T*-cell decay in vivo, J. Virol. 77 (2003) 5037.
[22] A.S. Perelson, P.W. Nelson, Mathematical analysis of HIV-1 dynamics in vivo, SIAM Rev. 41 (1999) 3.
[23] M. Louie, C. Hogan, M. Di Mascio, A. Hurley, V. Simon, J. Rooney, N. Ruiz, S. Brun, E. Sun, A.S. Perelson, D.D. Ho, M. Markowitz, Determining the relative efficacy of highly active antiretroviral therapy, J. Infect. Dis. 187 (2003) 896.
[24] G. Dornadula, H. Zhang, B. VanUitert, J. Stern, L. Livornese Jr., M.J. Ingerman, J. Witek, R.J. Kedanis, J. Natkin, J. DeSimone, R.J. Pomerantz, Residual HIV-1 RNA in blood plasma of patients taking suppressive highly active antiretroviral therapy, JAMA 282 (1999) 1627.
[25] M. Di Mascio, G. Dornadula, H. Zhang, J. Sullivan, Y. Xu, J. Kulkosky, R.J. Pomerantz, A.S. Perelson, In a subset of subjects on highly active antiretroviral therapy, human immunodeficiency virus type 1 RNA in plasma decays from 50 to <5 copies per milliliter, with a half-life of 6 months, J. Virol. 77 (2003) 2271.
[26] J.F. Lawless, Censoring and statistical methods, in: W. Shewart, S.S. Wilks (Eds.), Statistical Models and Methods for Lifetime Data, Wiley, New York, 1982, p. 31.
[27] M.R. Furtado, D.S. Callaway, J.P. Phair, K.J. Kunstman, J.L. Stanton, C.A. Macken, A.S. Perelson, S.M. Wolinsky, Persistence of HIV-1 transcription in peripheral-blood mononuclear cells in patients receiving potent antiretroviral therapy, New England J. Med. 340 (1999) 1614.
[28] J.K. Percus, O.E. Percus, M. Markowitz, D.D. Ho, M. Di Mascio, A.S. Perelson, The distribution of viral blips observed in HIV-1 infected patients treated with combination antiretroviral therapy, Bull. Math. Biol. 65 (2003) 263.
[29] M. Di Mascio, M. Markowitz, M. Louie, C. Hogan, A. Hurley, C. Chung, D.D. Ho, A.S. Perelson, Viral blips dynamics during HAART, J. Virol., in press.
[30] L. Ruiz, J. Martinez-Picado, J. Romeu, R. Paredes, M.K. Zayat, S. Marfil, E. Negredo, G. Sirera, C. Tural, B. Clotet, Structured treatment interruption in chronically HIV-1 infected patients after long-term viral suppression, AIDS 14 (2000) 397.
[31] L. Ruiz, G. Carcelain, J. Martinez-Picado, S. Frost, S. Marfil, R. Paredes, J. Romeu, E. Ferrer, K. Morales-Lopetegi, B. Autran, B. Clotet, HIV dynamics and *T*-cell immunity after three structured treatment interruptions in chronic HIV-1 infection, AIDS 15 (2001) F19.